

Analytical Study on Piezoelectric Effects on Exciton Dissociation

SeongMin Kim^{1,*,+}, Jaewook Ha², Hyeok Kim³ and Jin-Baek Kim²

¹ *The Office of the Theory & Modeling Based Design of Energy Harvesting (private lab), Maetan 3-dong, Yeongtong-gu, Suwon-si, Gyeonggi-do 443-373, Korea.*

² *Department of Chemistry, Korea Advanced Institute of Science and Technology, Daejeon 305-701, Korea.*

³ *Photo-Electronic Hybrids Research Center, Korea Institute of Science and Technology, Seoul 136-791, Korea.*

Received 14 May 2015; Accepted (in revised version) 16 November 2015

Abstract. We analytically and numerically compute the Onsager dissociation rate (exciton dissociation) on an interface induced by a piezoelectric potential in an inorganic-organic hybrid p-n junction system (ZnO + (poly(p-phenylene vinylene)); PPV). When a positive piezoelectric potential is created at the interface region owing to the deformation of the system, free electrons accumulate at the interface. Hence, screening effects are observed. It is assumed that the electron layer formed at the interface then attracts free holes from the p-type PPV region, which leads to exciton formation, possibly via the Langevin recombination process. The increased exciton density can then contribute to the Onsager dissociation rate, which is maximum around the interface. This paper focuses on the role of piezoelectric effects in promoting exciton formation at the interface and its relation with the exciton dissociation rate.

PACS: 71.35.-y, 77, 72.20.Jv, 73.40.Lq

Key words: Exciton dissociation, Onsager rate, piezoelectric, p-n junction, recombination.

1 Introduction

Dissociation of bounded electron-hole pairs (excitons) is important in organic solar cell devices [1, 2]. In a p-n junction system, a photo-generated exciton can migrate to the interface via diffusion. Then, owing to the potential difference (built-in potential plus applied bias) between each side of the interface, exciton dissociation, resulting in charge separation, can occur across the interface [1, 2]. Here, the dissociation of excitons can

*Corresponding author. *Email addresses:* smkim417@hotmail.com (S. M. Kim), hjaewook@kaist.ac.kr (J. Ha), fomalhout@gmail.com (H. Kim), jbkim21@kaist.ac.kr (J.-B. Kim)

[†]Current address: CAE, Platform Technology Lab, Samsung Advanced Institute of Technology.

be explained by Onsager's theory [3,4], where the dissociation rate constant (k_{diss}) [5] is given by,

$$k_{diss} = \frac{\gamma}{\frac{4}{3}\pi a^3} e^{-E_b/k_B T} \left[1 + b + \frac{b^2}{3} + \frac{b^3}{18} + \frac{b^4}{180} + \dots \right]. \quad (1.1)$$

In Eq. (1.1), E_b is the exciton binding energy, $b = q^3 |\vec{\nabla} \phi| / 8\pi\epsilon k_B^2 T^2$ is the field parameter, k_B is the Boltzmann constant, T is the temperature, γ is the Langevin recombination parameter, given by $\frac{q}{e}(\mu_n + \mu_p)$ [6] and a is the electron-hole pair distance. Then, the Onsager dissociation rate D [3,4] is given by,

$$D = k_{diss} \cdot X \quad (1.2)$$

$$= \frac{\gamma}{\frac{4}{3}\pi a^3} e^{-E_b/k_B T} \left[1 + b + \frac{b^2}{3} + \frac{b^3}{18} + \frac{b^4}{180} + \dots \right] X, \quad (1.3)$$

where X is the exciton density.

The calculation of D requires various parameters such as b , X , γ , E_b , a , k_B and T . Among them, the field parameter b is associated with the electric field, which is related to the piezoelectric field/potential induced at the p-n interface in the hybrid junction system when the system is deformed.

In this case, electrons or holes around the interface can accumulate at the interface, if the piezoelectric field is strong enough even a depletion zone is formed. The piezoelectric charges resulting in piezoelectric fields are not newly created ones but are resulted from an occurrence of non-zero dipole moments which are generated by the deformation of the structures of the piezoelectric materials using the external forces exerted onto the system. (There is no change in total number of charges). Around such piezoelectric charges generated, free carriers can be accumulated into them and screen them to reduce the piezoelectric potential or can conserve them to maintain the piezoelectric potential.

Excitons can be formed via the exciton recombination process (Langevin recombination) [7,8], by controlling the free carriers collected at the interface, resulting from the piezoelectric potential induced. In this way, the density of excitons (and ultimately, the dissociation rate) can be controlled, as the piezoelectric field can affect both b and X . This is a point of modeling excitons here, but there are yet no experimental papers measuring such a phenomenon of exciton formation induced by the piezoelectric effects in a hybrid p-n junction system.

In this paper, we first analytically solve the Onsager dissociation rate in the inorganic hybrid p-n junction structure where a positive piezoelectric potential is generated on the p-n interface, which leads to accumulation of electrons that then assist in forming excitons. These excitons are then dissociated into free carriers. We calculate the Onsager dissociation rate numerically to better understand the piezoelectric effects on the exciton dissociation in the hybrid p-n junction system and obtain a better physical insight into it.

2 Analytical solution for 1D inorganic-organic hybrid p-n junction system

2.1 Hybrid p-n junctions

To describe a hybrid p-n junction, the Shockley theory [9] along with the exciton equation [7, 8] is used. Here, we assume that the p-type material is a non-piezoelectric poly(p-phenylene vinylene) (PPV) [10,11] and the n-type material is a piezoelectric ZnO material [12, 13] (as shown in Fig. 1(a)). The growth direction of ZnO is indicated along the c-axis in the figure. The positive piezoelectric charges are created at the interface mostly at the n-ZnO part of the junction system by elongation along the c-axis because the piezoelectric charge density arises from the piezoelectric properties of n-ZnO. It is assumed that the distribution of the positive piezoelectric charges around the junction is within the width w_p in n-ZnO part, as shown in Fig. 1(a).

In our model, an abrupt junction consisting of impurities – N_D (donor concentration) and N_A (acceptor concentration) is used initially. However, when the increasing positive piezoelectric charges are generated, electrons from n-ZnO start to remove the donors (positive density) until only the electron density remains within a width of $w_e - w_p$, as shown in Fig. 1(b). In the p-type PPV region, holes form a depletion zone, which is indicated by a box representation (N_A) within a width of w_A , assuming that PPV is crystalline. To calculate the accumulated electron density n_e due to the positive piezoelectric potential induced at the interface inside the p-n junction, the electric field and potential distribution are first considered. In the case of a 1D hybrid p-n junction ZnO-PPV system, the Poisson equation can be written as,

$$\frac{dE}{dx} = \frac{\rho(x)}{\epsilon_s} = \frac{1}{\epsilon_s} [-qN_A(x) + \rho_{piezo}(x) - qn_e(x) - qn(x) + qp(x)], \quad (2.1)$$

where $N_A(x)$ is the acceptor concentration, $\rho_{piezo}(x)$ is the density of piezoelectric charges, $n_e(x)$ is the accumulated free electron density around the interface, $n(x)$ is the free electron density, $p(x)$ is the free hole density, w_A is the depletion width in the p type region, w_p is the width of the positive piezoelectric charge density, and $w_e - w_p$ is the width of the accumulated electron density beside the ρ_{piezo} around the interface as shown in Fig. 1(b). The electric field is then calculated by integrating $\rho(x)/\epsilon_s$ in Eq. (2.1)

$$E(x) = \frac{-qN_A}{\epsilon_s}(x + w_A) \quad \text{for } -w_A \leq x \leq 0, \quad (2.2)$$

$$E(x) = \frac{1}{\epsilon_s}\rho_{piezo}(x - w_p) - \frac{qn_e}{\epsilon_s}(w_p - w_e) \quad \text{for } 0 \leq x \leq w_p, \quad (2.3)$$

$$E(x) = \frac{-qn_e}{\epsilon_s}(x - w_e) \quad \text{for } w_p \leq x \leq w_e. \quad (2.4)$$

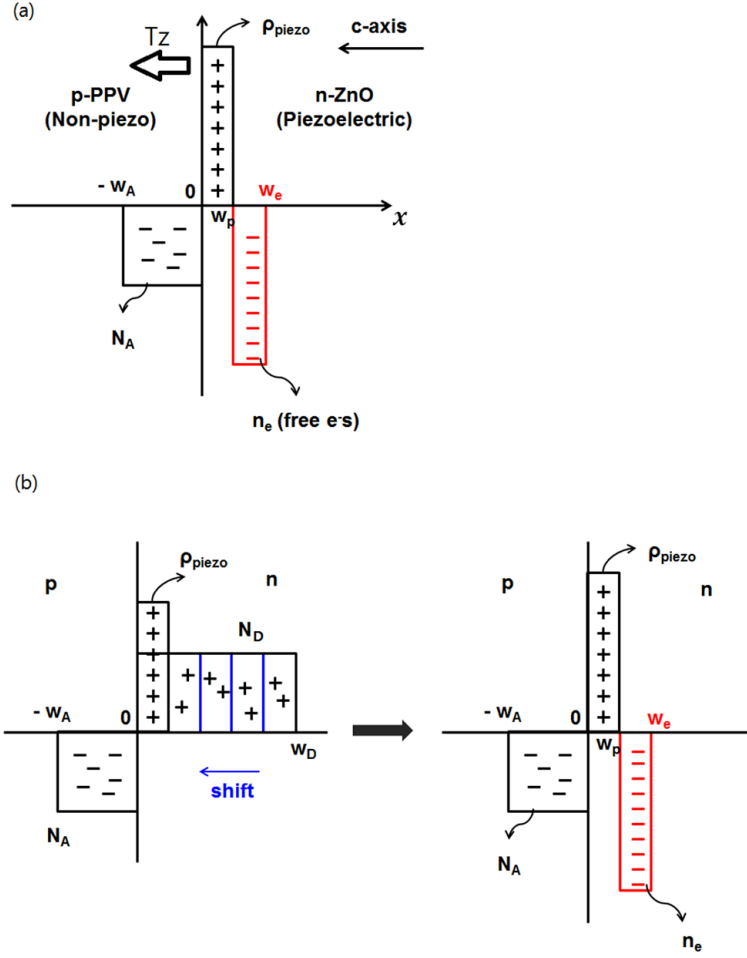


Figure 1: (a) Inorganicorganic hybrid p-n junction structure, with positive piezoelectric charge density due to elongation along the c-axis. Piezoelectric charge density ρ_{piezo} , acceptor concentration N_A , and collected electrons n_e are indicated. (b) Initially, both donors (N_D) and acceptors (N_A) present with the piezoelectric charge density ρ_{piezo} (left). However, as ρ_{piezo} increases, the donor concentration starts to reduce due to increase in free electron density around the interface (right).

From the above electric fields, the electric potential Φ can be obtained as shown below,

$$\Phi(x) = \frac{qN_A}{\epsilon_s} \left\{ \frac{1}{2}x^2 + w_A x \right\} + \frac{qN_A w_A^2}{2\epsilon_s} \quad \text{for } -w_A \leq x \leq 0, \quad (2.5)$$

$$\Phi(x) = - \left\{ \frac{1}{\epsilon_s} \rho_{piezo} \frac{x^2}{2} - \frac{1}{\epsilon_s} \rho_{piezo} w_p x - \frac{qn_e}{\epsilon_s} (w_p - w_e) x \right\} + \frac{qN_A w_A^2}{2\epsilon_s} \quad \text{for } 0 \leq x \leq w_p, \quad (2.6)$$

$$\Phi(x) = \frac{qn_e}{\epsilon_s} \left(\frac{x^2}{2} - w_e x \right) + \frac{1}{\epsilon_s} \rho_{piezo} \frac{w_p^2}{2} + \frac{qn_e}{\epsilon_s} \frac{w_p^2}{2} + \frac{qN_A w_A^2}{2\epsilon_s} \quad \text{for } w_p \leq x \leq w_e. \quad (2.7)$$

Therefore, the built-in potential Φ_{bi} can be obtained as shown below,

$$\Phi_{bi} = \frac{qn_e}{\epsilon_s} \left(\frac{-w_e^2}{2} \right) + \frac{1}{\epsilon_s} \rho_{piezo} \frac{w_p^2}{2} + \frac{qn_e}{\epsilon_s} \frac{w_p^2}{2} + \frac{qN_A w_A^2}{2\epsilon_s}. \quad (2.8)$$

From the built-in potential, the accumulated electron density n_e can be calculated from the piezoelectric potential induced as follows:

$$n_e = \left\{ \Phi_{bi} - \frac{1}{\epsilon_s} \rho_{piezo} \frac{w_p^2}{2} - \frac{qN_A w_A^2}{2\epsilon_s} \right\} \cdot \frac{2\epsilon_s}{q(w_p^2 - w_e^2)}. \quad (2.9)$$

Then, the maximum density of the excitons X can be estimated as

$$X^{\max} = 2 \cdot n_e. \quad (2.10)$$

The Onsager dissociation rate can be restated as shown below,

$$D \cong \frac{\gamma}{\frac{4}{3}\pi a^3} e^{-\frac{E_b}{k_B T}} \left[1 + b + \frac{b^2}{3} + \dots \right] \times 2n_e, \quad (2.11)$$

where b is given by the following equations,

$$b = \frac{q^3}{8\pi\epsilon_s k_B^2 T^2} \left| \frac{-qN_A}{\epsilon_s} (x + w_A) \right| \quad \text{for } -w_A \leq x \leq 0, \quad (2.12)$$

$$b = \frac{q^3}{8\pi\epsilon_s k_B^2 T^2} \left| \frac{1}{\epsilon_s} \rho_{piezo} (x - w_p) - \frac{qn_e}{\epsilon_s} (w_p - w_e) \right| \quad \text{for } 0 \leq x \leq w_p, \quad (2.13)$$

$$b = \frac{q^3}{8\pi\epsilon_s k_B^2 T^2} \left| \frac{-qn_e}{\epsilon_s} (x - w_e) \right| \quad \text{for } w_p \leq x \leq w_e. \quad (2.14)$$

3 Results and discussion

3.1 Numerical simulation of hybrid p-n junctions

The equation of the inorganicorganic p-n junction system, consisting of charge transport with exciton dissociation in the steady state, is described in [14]. The analytical expression for the Onsager dissociation rate in Eq. (2.11), in the case of a 1D p-n junction, shows a correlation between the piezoelectric potential and the exciton density, and thus can be used to obtain the dissociation rate. In other words, it can provide a mechanism of how the piezoelectric potential can affect the dissociation rate and a physical insight into the system. Based on this, the equations governing the exciton behavior for the junction system can be numerically solved. The region of exciton dissociation is constrained to the vicinity of the junction interface. For recombination of carriers, the Langevin recombination for the formation of excitons [7,8] and the Shockley-Read-Hall (SRH) recombination

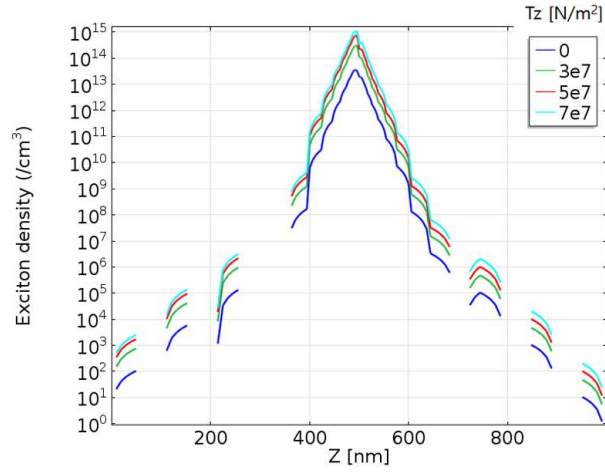


Figure 2: Exciton density distribution along the z-axis for different T_z .

for traps [9] are both considered. The trap level in SRH recombination is modeled such that it lies in the middle of forbidden band gap. As a boundary condition of the electrical contacts, the bottom of the p-n junction is grounded, and the top potential is set to be -0.6 V, with ideal ohmic contacts. The boundary condition used is a fixed boundary condition (i.e., Dirichlet boundary condition) [15].

Fig. 2 shows the exciton density along the z-axis where the density is maximum around the interface (at 500 nm). It can be clearly seen that the exciton density in the presence of $T_z > 0 \text{ N/m}^2$ is greater than that with no compression ($T_z = 0$), owing to the induced piezoelectric potential at the interface. Note that even with $T_z = 0$ (reference), exciton exists because the free carriers (electrons and holes) are still present in the junction region. In other words, because the density of electrons and holes is not completely zero, there is a possibility of exciton formation via recombination processes, even in the depletion zone. The gap in Fig. 2 seems to originate from unstable meshes which cannot calculate appropriate values at the points. The value of the exciton density should have positive values, so that it can be meaningful physically. As explained previously, here the excitons are generated not by incident light, but by piezoelectric potential which attracts free carriers (electrons and holes) to form excitons due to a possibility that electrons and holes can meet each other. Therefore, the source of origin of the generation of the excitons is different from the conventional organic solar cell where the excitons are created everywhere where light is incident on the cell. However, the device model used here is based on the p-n junction solar cell device, not an OLED model.

Fig. 3 shows the distribution of b along the z-axis, indicating a maximum around the p-n interface with different T_z . In Eq. (2.11), the polynomial form of the field parameter is also calculated in the equation and shown in the Fig. 4 with different T_z . The value of $b(\frac{q^3 |\vec{E}|}{8\pi\epsilon k_B^2 T^2})$ is greater when $T_z > 0$, because $|\vec{E}|$ is influenced by the piezoelectric field

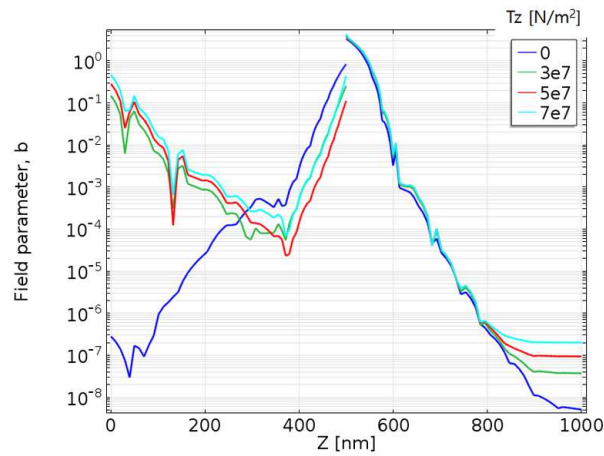


Figure 3: Distribution of the field parameter b along the z -axis for different T_z .

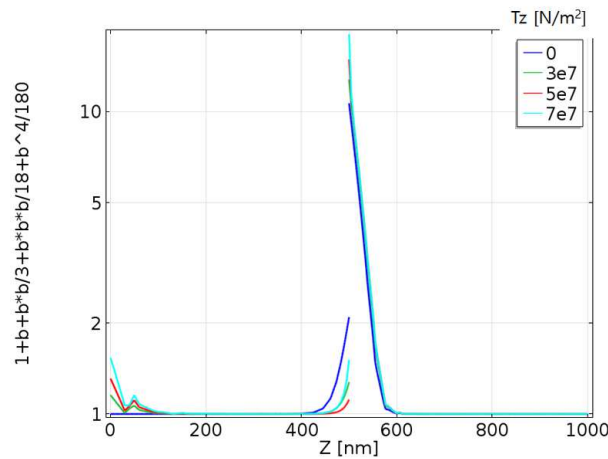


Figure 4: Polynomial of the distribution of the field parameter along the z -axis for different T_z .

induced at the interface.

Fig. 5 shows the distribution of the Onsager dissociation rate along the z -axis with positive piezoelectric potential induced at the interface ($T_z > 0N/m^2$), where the maximum is indicated at the junction, and is compared with the no-elongation case in the model system ($T_z = 0N/m^2$). The plot of the dissociation rate is quite similar to that of the exciton density. This proves the fact that the exciton density is a dominant parameter in determining the dissociation rate, as shown in Eq. (1.3). The reason for the maximum is that the positive piezoelectric potential can promote exciton formation by generating positive piezoelectric charges at the interface. This then attracts the electrons, followed by holes, which leads to the formation of excitons, as shown in Fig. 6. Thus, the increase in exciton density contributes to the increase in the dissociation rate. Note that the order of

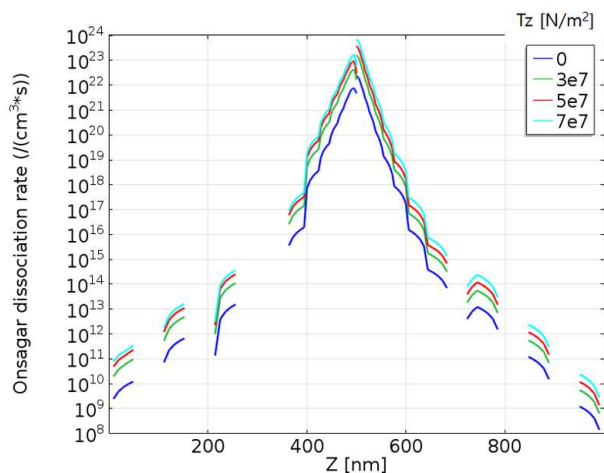


Figure 5: Distribution of the Onsager dissociation rate along the z-axis for different T_z .

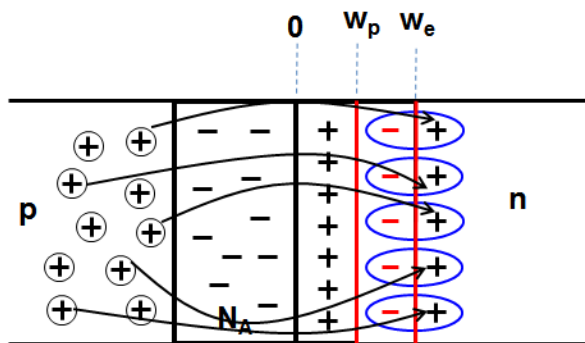


Figure 6: A schematic of exciton formation around the interface due to the piezoelectric charges, where the free electrons that are formed in the n-type region attract free holes from the p-type region.

the b is lesser than that of the exciton density. This implies that the dominant parameter in the exciton dissociation rate is not b , but X .

4 Conclusion

In summary, we present an analytical model and a numerical study on the exciton dissociation rate of the hybrid p-n junction system under elongation. Our analytical approach to describe the exciton dissociation using the piezoelectric potential is useful for understanding the piezoelectric effects on carrier separation. The numerical results from the model system are useful to understand that the exciton dissociation is maximum around the junction. This is because of the exciton density. The model study introduced here can

be used to establish a foundation to design a piezophototronic device using the piezoelectric potential, which will be able to control both exciton density and exciton dissociation. The future work is following: This model can be applicable to the entire organic solar cell model [16] to fully analyze the device performance.

Acknowledgments

This research was supported by the Office of the Theory & Modeling Based Design of Energy Harvesting, Korea.

References

- [1] Tang, C. W. Appl. Phys. Lett. 1986, 48, 183.
- [2] Sariciftci, N. S., Smilowitz, L., Heeger, A. J. and Wudl, F. Science 1992, 258, 1474.
- [3] Goliber, T. E. and Perlstein, J. H., J. Chem. Phys. 1984, 80, 4162.
- [4] Barker, J. A., Ramsdale, C. M. and Greenham, N. C., Modeling the current-voltage characteristics of bilayer polymer photovoltaic devices, Phys. Rev. B 2003, 67, 075205.
- [5] Braun, C. L., J. Chem. Phys. 1984, 80, 4157.
- [6] Van der Holst, J. J. M., Van Oost, F. W. A., Coehoorn, R. and Bobbert, P. A. Phys. Rev. B, 80, 235202.
- [7] Kodali, H. K. and Ganapathysubramanian B. Modelling Simul. Mater. Sci. Eng. 2012, 20, 035015.
- [8] Buxton, G. A. and Clarke N., Modelling Simul. Mater. Sci. Eng. 2007, 15, 1326.
- [9] a) Sze, S. M. Physics of Semiconductor Devices, 2nd ed., Wiley, New York, 1981; b) Schottky, W. Naturwissenschaften 1938, 26, 843; c) Bethe, H. A., MIT Radiat. Lab. Rep., 1942, 43, 12; d) Crowell, C. R. and Sze, S. M. Solid-State Electron. 1966, 9, 1035.
- [10] O. Schafer et al., Poly(p-phenylenevinylene) by chemical vapor deposition, Synthetic Metals 1996, 82, 1.
- [11] Karabacak, T., Wiegand, C., Senkevich, J. J., Lu, T.-M., Jia, D. and Fernandez, F., Enhanced photoluminescence of PPV thin film coated on the nano-structured substrate by glancing angle deposition, Electrochemical and Solid-State Letters, in press.
- [12] Gao, Y. and Wang, Z. L. Nano Lett. 2007, 7, 2499.
- [13] Gao, Y. and Wang, Z. L. Nano Lett. 2009, 9, 1103.
- [14] Kim, S. M., Piezoelectric effects on the exciton dissociation rate in the organic-inorganic hybrid system, Integrated Ferroelectrics: An International Journal (accepted).
- [15] Zhang, Y., Liu, Y. and Wang, Z. L., Adv. Mater. 2011, 19;23(27):3004-13.
- [16] Buxton, B. Alternative Energy Technologies: An Introduction with Computer Simulation, CRC press, 2014